Volume 4, No. 1, 1993

Journal of the Faculties of
Engineering of Uludağ University

TURBULENT FLOWS IN ANNULAR DUCTS

Habib UMUR*

ABSTRACT

Skin friction factors, mean and secondary flow velocities together with normal and Reynolds stresses were measured in an eccentric annular duct (eccentricity of unity) with a Newtonian fluid at Reynolds numbers of 9000 and 26600 which ensured turbulent and fully developed turbulent flows. The three components of mean and rms velocities were recorded by the use of laser Doppler velocimeter with a refractive index matching technique.

Static pressure distribution was smaller (up to 15%) than asmooth pipe and near wall velocities deviated from the law of the wall up te 5 %. The location of maximum velocity and zero shear stress occurred at the same locations within the measurement accuracy. The secondary flow velocities of less than 2% of the bulk velocity showed two cells of circulation at each side of the symmetry.

ÖZET

Eş ve Ayrı Merkezli Kanallarda Turbulanslı Akış

Sürtünme katsayıları, ortalama ve ikincil akış hızları, normal ve Reynolds gerilmeleri eksantrik bir kanalda turbulanslı ve tam gelişmiş türbulanslı (Re = 9000 ve 26600) akış durumunda ölçülmüştür. Üç yöndeki hız bileşenleri ve türbulans yoğunlukları laser Doppler hızölçer ile "Refractive index matching" yöntemi kullanılarak belirlenmiştir.

---

* *Yard. Doç. Dr.; U.Ü. Mühendislik-Mimarlık Fakültesi, Makina Bölümü.*

Statik basınç dağılımı pürüzsüz bir boru akışından % 15 daha az, duvara yakın yerdeki hızlar ise logaritmik hız profilinden % 5 nispetinde bir sapma göstermiştir. Maksimum hız ve sıfır kesme gerilmeleri, ölçüm hataları içinde, yaklaşık aynı yerlerde oluşmuştur. Aksiyal yöndeki hızın % 2'si kadar olan ikincil akışlar, simetri ekseninin her iki yanında iki ayrı sirkülasyon oluşturacak şekilde gözlenmiştir.

1. INTRODUCTION

In oil drilling, the drill shaft may touch to the well casing after some distance downstream and may cause different flow characteristics so that measurements were obtained at the extreme case of eccentricity of unity with a Newtonian fluid (a mixture of 31.8% tetraline in turpentine).

Jonsson and Sparrow (1966) and Kacker (1973) have examined eccentric annulus flows and the results show, for example, that the friction factor decreased with increasing eccentricity by up to 7 %, that the near wall flows deviated from the law of the wall, particularly at the inner wall where curvature can be important, and that a double-cellular structure existed with maximum secondary flow velocity of around 0.02 of the bulk flow velocity with a diameter ratio of 0.17 and an eccentricity of 0.47, defined by $e = 1/(R_0-R_i)$ with 1 the distance between the centers of the inner and outer pipes and R_i and R_0 are inner and outer radius. The measurements of Nouri, Umur and Whitelaw (1992) have shown that the general arrangements of the annulus flows are likely to lead to an investigation of the touching walls (eccentricity of unity) so that these measurements have been carried out with a mixture of 31.8 % tetraline in turpentine in order to use laser Doppler velocimetry without limitations imposed by refraction. For this purpose, constant temperature of $25 \pm 0.02^{\circ}C$ was maintained throughout the experiments.

The present Newtonian flows correspond to bulk flow Reynolds numbers of 9000 and 26600 with a diameter ratio of 0.5 and an eccentricity of unity. The major purpose of the present investigation was to show, how the fluid properties influence the flow at an eccentric arrangement of unit eccentricity, so as to guide the development of oil drilling arrangements where the initial pressures involve fluids with Newtonian and non-Newtonian characteristics. The flow configuration and instrumentation are described briefly in the following section and results presented and discussed in section. This paper ends with a summary of the more important findings in section [4].

2. FLOW CONFIGURATİON AND INSTRUMENTATION

Measurements were obtained in an eccentric annuli duct at Imperial College of Science, Technology and Medicine, shown of figure 1 with the details

of the test section and coordinate system, which consists of a centrifugal pump to deliver fluids from a supply tank through a section of honeycomb and contraction tho the annular passage. The distance between the centres of the inner shaft and the outer pipe was 10 mm which gave an eccentricity of unity with a diameter ratio, of outer pipe of nominal inside diameter (40.3 mm) to inner rod diameter (20.1 mm), of 0.5. The rig has already been used by Nouri et al. (1992) who documented Newtonian and non-Newtonian flow characteristics in concentric and eccentric (eccentricity of 0.5) annuli.

The bulk flow was measured by a calibrated orifice plate with precision better than 3 %. The temperature of the Newtonian fluid was controlled to 25.0 ± 0.02°C so that its refractive index was 1.489, identical to that of the plexiglass material used to form the test section. The bulk flow conditions and properties are given in table 1. Static pressures were measured with holes of 0.5 mm diameter distributed longitudinally and circumferentially in the outer diameter. They were read from a calibrated manometer bank with ±1 mm resolution. The specific gravity of the manometer fluid was 1880 kg/m^3 giving a height range of 20 to 400 mm.

Table: I. Flow Properties For a Mixture of 31.8 % tetraline in turpentine

Outer diameter (D_0, mm)		40.3	
Inner diameter (D_{in}, mm)		20.1	
Hydraulic diameter (d_h, mm)		20.2	
Mass flow rate (x10^{-3}, m^3/s)	0.68		2.05
Bulk velocity (U_b, m/s)	0.72		2.15
Reynolds number (Re, x10^3)	9.0		26.6

Fluid mixture temperature (°C)	25 ± 0.02
Density of mixture (ρ, kg/m^3)	896
Kinematic viscosity of mixture (ν, x10^{-6} m^2/s)	1.62
Refractive index of the mixture at λ = 632.8 (nm)	1.489

Three components of the mean, rms and secondary flow velocities were measured by a Laser Doppler velocimeter described by Umur (1991). The optical configuration is shown in figure 2. The light source was a 5 mW He-Ne laser (Spectra Physics 120) with a 632.8 nm wavelength and 0.65 mm unfocussed beam diameter at the e-^{2} intensity level. The laser beam was focused by a plano-convex lens (f_1) onto the radial diffraction grating (Technish Physische Dienst, type H), where it was diffracted into the zero order and pairs of higher order beams. The grating could be rotated at constant angular velocities to provide frequency shifts up to 5.5 MHz, positive or negative, enablign directional

discrimination and ensuring that the Doppler signal was in the optimum frequency band of the processing instrumentation. The two first order beams were collimated by a plano convex lens (f_2) and then focussed by a second plano-convex imaging lens (f_3) to form the measuring volume. The best uniformity of the fringe spacing (d_f) and the smallest size of the measuring volume occurred when the two first order beams intersected at their waist. The dimensions of the measuring volume of figure 2, can be defined as the minor axis, $b_x=b_s/\cos(\theta)$, the major axis, $b_y=nb_s/\sin(\theta)$, the number of fringes ($N=b_x/d_f$); where b_s ($=4\lambda f_1 f_3/[\pi b_0 f_2]$, is the beam diameter of the measuring volume, θ is the half angle of the intersection beams and n is the refraction index of the fluid. The fringe spacing (d_f) is given by

$$df = \lambda / 2 \sin(\theta) \qquad (1)$$

which facilitates the conversion of the Doppler frequency directly to the fluid velocity.

The light scattered by the particles from the measuring volume was focussed onto a pinhole located in front of photomultiplier (EMI 9817). The amount of scattered lights on the photomultiplier could be controlled dby the collecting lens (f_4) equipped with an adjustable aperture. The characteristics of the optical system are summarised in table 2.

Table: 2. Characteristics of The Optical System

Laser power, mW	5
Laser wavelength, λ, nm	632.8
Focal length of focusing lens, f_1, mm	60
Focal length of collimating lens, f_2, mm	300
Focal length of imaging lens, f_3, mm	200 and 300
Focal length of collecting lenss, f_4, mm	150
Measured half angle of beams, θ, degrees	8.92 and 6.05
Laser beam diameter at laser output, b_0, mm	0.65
Laser beam diameter at the measuring volume, b_s, mm	0.4 and 0.6
Intersection volume diameter at e^{-2} intensity, b_x, μm	40 and 60
Intersection volume length at e^{-2} intensity, b_y, μm	250 and 575
Fringe spacing, d_f, μm	2.04 and 3.04
Number of fringes in measuring volume, N	20

The output of the photomultiplier was amplified and high-pass filtered to remove the low frequency pedestal and low frequency noise, and a low pass filter avoided high frequency noise. The conditioned signal output was monitored on an

oscilloscope (Tektronix 2225, 50 MHz) for display and input to a purpose built frequency counter. The Doppler bursts were counted by a digital counter controlled by the trigger output of the oscilloscope, in order to count each Doppler signal once only and to operate with a preset discrimination level. The frequency of a Doppler signal was measured by timing of the duration of the signal burst over a specified number of cycles by a high frequency clock, here the measurements were made using 16 cycles of each burst. Two threshold levels discriminated the Doppler burst signals from the noise, and the signal timing was activated only if the signal amplitude exceeded both levels and, if the difference between the frequency measured above and below the discrimination level exceeded a preset value (0.19 %) of the measured frequency, the measurement was rejected so as to reduce the possibility of measuring noisy Doppler bursts. The frequency counter was interfaced to a microprocessor (Apple IIe) where the binary coded decimal values generated by the counter were processed to yield decimal frequency values. The individual Doppler frequencies were processed to yield ensemble-averaged mean and rms velocities which corresponded to time averaged quantities.

3. RESULTS AND DISCUSSION

Velocity results, normalised with bulk velocities (U_b) and maximum velocities (U_m), are presented separately for planes 2, 3 and 4. Distances are normalised with the radial distance from the outer to inner wall. The dimensions for the eccentric arrangement of unity is shown in figure 1(b).

The measurement of static pressure gradient of figure 3 was found to be 3 to 16 % smaller in the regions of Reynolds number from $3x10^3$ to $3x10^4$ than that of the smooth circular pipe relationship suggested by Rothfus (1948)

$$C_f = 0.087\ Re^{-0.25} \tag{2}$$

and the skin friction factors decreased with increasing eccentricity and reached the lowest value at unit eccentricity. The experimental skin friction factor is determined by

$$C_f = (dP/dx)\ (d_h / 2\rho\ U_b^2) \tag{3}$$

where dP/dx is the static pressure difference, d_h is the hydraulic diameter, U_b is the bulk flow velocity and ρ is the density of the liquid.

Mean velocity profiles for the two Reynolds numbers of 26600 and 9000 were measured on three planes, which correspond to a symmetrical and fully developed flow and show that the velocity maximum was located towards the

inner wall at plane 3 and towards the outer wall in planes 2 and 4. The variations of the mean velocity profiles of figure 4(a) and (b) are considerable with the maximum veolcities in planes 2 to 4 corresponding to 1.25, 1.42 and 1.27, and to 1.30. 1.53 and 1.31 of the bulk velocities with the maximum difference of 14 % and 18 % between plane 2 and plane 3 at Reynolds numbers of 26600 and 9000 respectively. The difference in maximum velocities in planes 2 and 4 for both cases are almost negligible within the measurement precision.

The fluctuation velocities behaved as expected with magnitudes decreasing from axial, to circumferential, to radial components. The turbulence intensities and shear stresses of figure 5 also vary with circumferential location so that the turbulence intensities are largest in plane 3. The maximum shear stress in plane 3 is also the biggest of the three planes. In all cases, the profiles of shear stress become zero at locations which correspond to the middle of the gap, within the measurement precision. The shear stress coefficient, $u'v'/U_b^2$, has an extensive linear region in plane 3, with maximum of 3.3×10^{-3} at Reynolds number of 26600 and 4.5×10^{-3} at Reynolds number of 9000 which are 30 % higher than those of Nouri, Umur and Whitelaw (1992), and has sinusoidal variations at planes 2 and 4, which show fully turbulent flow at the largest gap.

The wall shear stress at the outer wall calculated from pressure measurements and presented in Clauser coordinates, and the zero shear stress locations with the equation:

$$\tau_0 = -(dP/dx)\,([R_0^2 - R_m^2] / 2R_0) \qquad (4)$$

where τ_0 is the outer wall shear stress and R_m is the location of zero shear stress. It is evident from figure 6 that the two Reynolds numbers lead to near-wall profiles which posses a logarithmic region similar to that of the accepted law of the wall with a deviation of around 5 %. The lines in figure 6 respectively represent the viscous sublayer, $U^+ = Y^+$, the law of the wall by Clauser (1956), $U^+ = 2.441\ \ln Y^+ + 4.9$, where $U^+ = U/u^*$ and $Y^+ = u^*y/\nu$, in which u^* is the friction velocity $(\tau_w/p)^{1/2}$. The detailed information at each plane is presented in table 3.

Secondary flow velocities of figure 7 were measured with a Bragg Cell unit at the Reynolds number of 26600, that shows two cells of circulation on either side of the plane of symmetry for the annuli of unit eccentricty, similar to those of Brundett and Baines (1964), with a maximum value of around 2 % of the bulk velocity, and that flows from the widest side to the narrowest side for the eccentricity of 0.5 with a maximum value of 1.5 % of the bulk velocity. The secondary flows were generated in such a way that they took the fluid from the high momentum region to the low momentum region. It is known from other non-circular duct flows, for example the square duct of Melling and Whitelaw (1976), that the differences between the two cross-stream normal stresses ($v'^2 - w'^2$) can cause secondary flows up to around 1.5 % of the maximum streamwise velocity and Kacker (1973) measured secondary flow velocities of the order of 1 % of the

mean velocity in a circular pipe containing one or two rods located with eccentricity of 0.475 and radius ratio of 0.175.

Table: 3. Circumferential Variation of Maximum Velocity

	Bulk Reynolds Number	Plane 2	Plane 3	Plane 4	U_{m2} / U_{m3}
U_m (m/s)	9000	0.942	1.105	0.949	0.852
Local Re		9930	13800	9970	
u* (m/s)		0.0546	0.0585	0.0545	
U_m (m/s)	26600	2.680	3.056	2.730	0.875
Local Re		28820	38100	28730	
u* (m/s)		0.133	0.143	0.133	

4. CONCLUSIONS

The results obtained at Reynolds numbers of 9000 and 26600 are in accord with expectations and provide evidence of the measurement accuracy. The maximum axial velocities varied circumferentially from 1.25 to $1.42U_b$, that the near-wall flow deviated from the law of the wall and the skin friction coefficient decreased with increasing eccentricity. There are two cells of circulation at each side of the symmetry with velocities less than around $0.02U_b$.

REFERENCES

1. BRUNDETT, E. and BAINES, W.D.: "The Production and Diffusion of Vorticity in Duct Flow", J. Fluid Mech., Vol. 19, p. 375, 1964.
2. CLAUSER, F.H.: "The Turbulent Boundary Layer", Advances in Applied Mechanics, Vol. 4, p. 1, 1956.
3. JONSSON, V.K. and SPARROW, E.M.: "Experiments on Turbulent Flow Phenomena in Eccentric Annular Ducts", J. Fluid Mech., Vol. 25, p. 65, 1966.
4. KACKER, S.C.: "Some Aspects of Fully Developed Turbulent Flow in Non-Circular Ducts", J. Fluid Mech., Vol. 57, p. 583, 1973.
5. MELLING, A. and WHITELAW, J.H.: "Turbulent Flow in a Rectangular Duct", J. Fluid Mech., Vol. 78, p. 289, 1976.
6. NOURI, J.M., UMUR, H. and WHITELAW, J.H.: "Flow in Concenric and Eccentric Annuli", Paper Submitted for Journal of Fluid Mechanics, 1992.
7. ROTHFUS, R.R.: "Velocity Distribution and Fluid Friction in Concentric Annuli", PhD Thesis, Carnegie Institute of Technology, 1948.
8. UMUR, H.: "Flows with Curvature", PhD Thesis, Imperial College, London University, 1991.

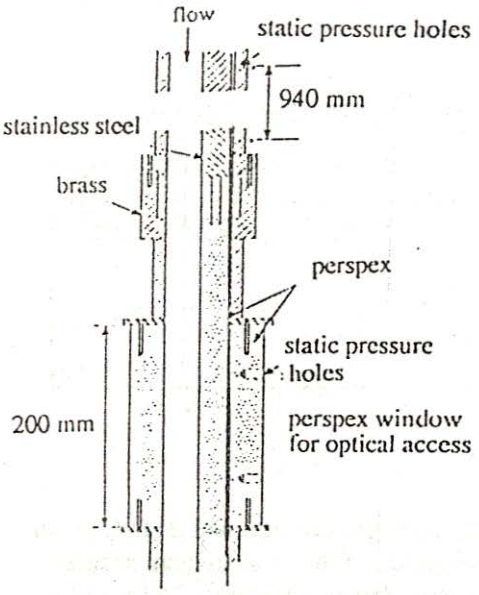

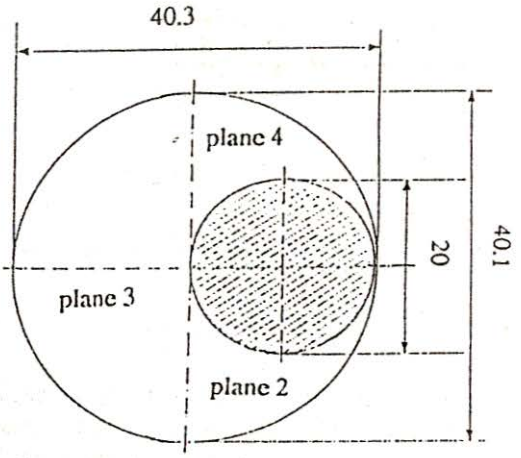

Figure: 1a. Annular pipe test section Figure: 1b. Dimensions for eccentric geometry

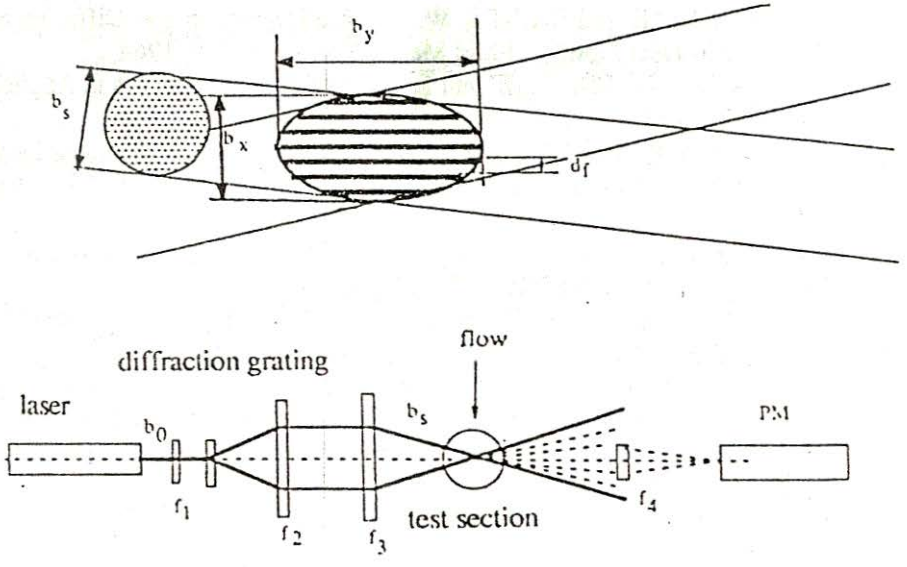

Figure: 2. Laser Doppler velocimeter

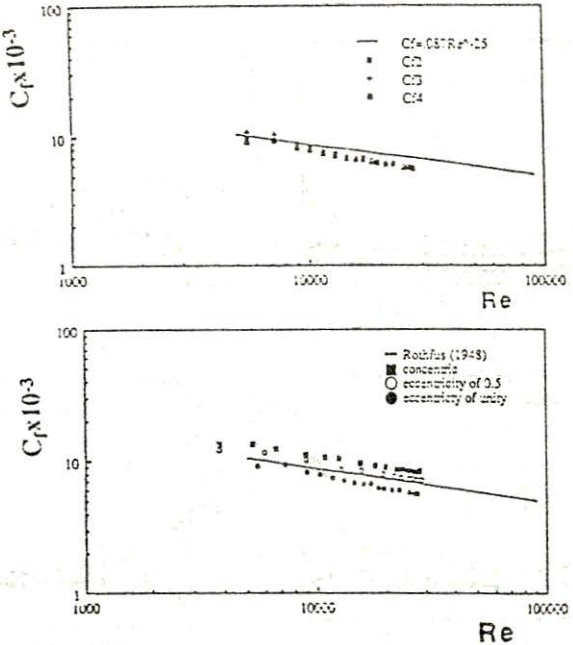

Figure: 3. Skin friction factors versus Reynolds number

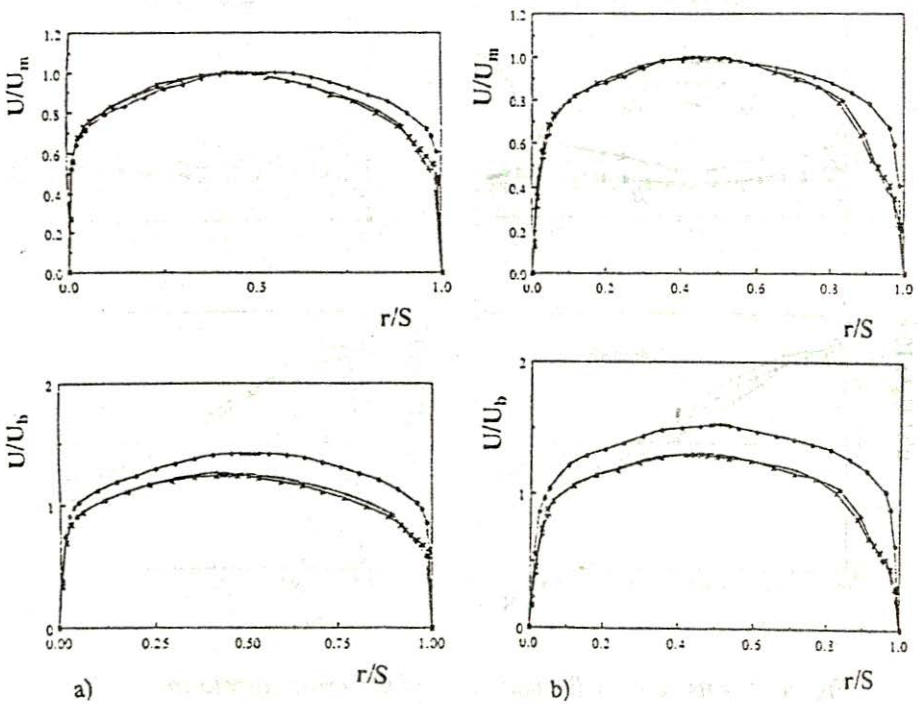

Figure: 4. Axial mean velocities; a) Re = 26600, b) Re = 9000
x plane 2, ◆ plane 3, + plane 4

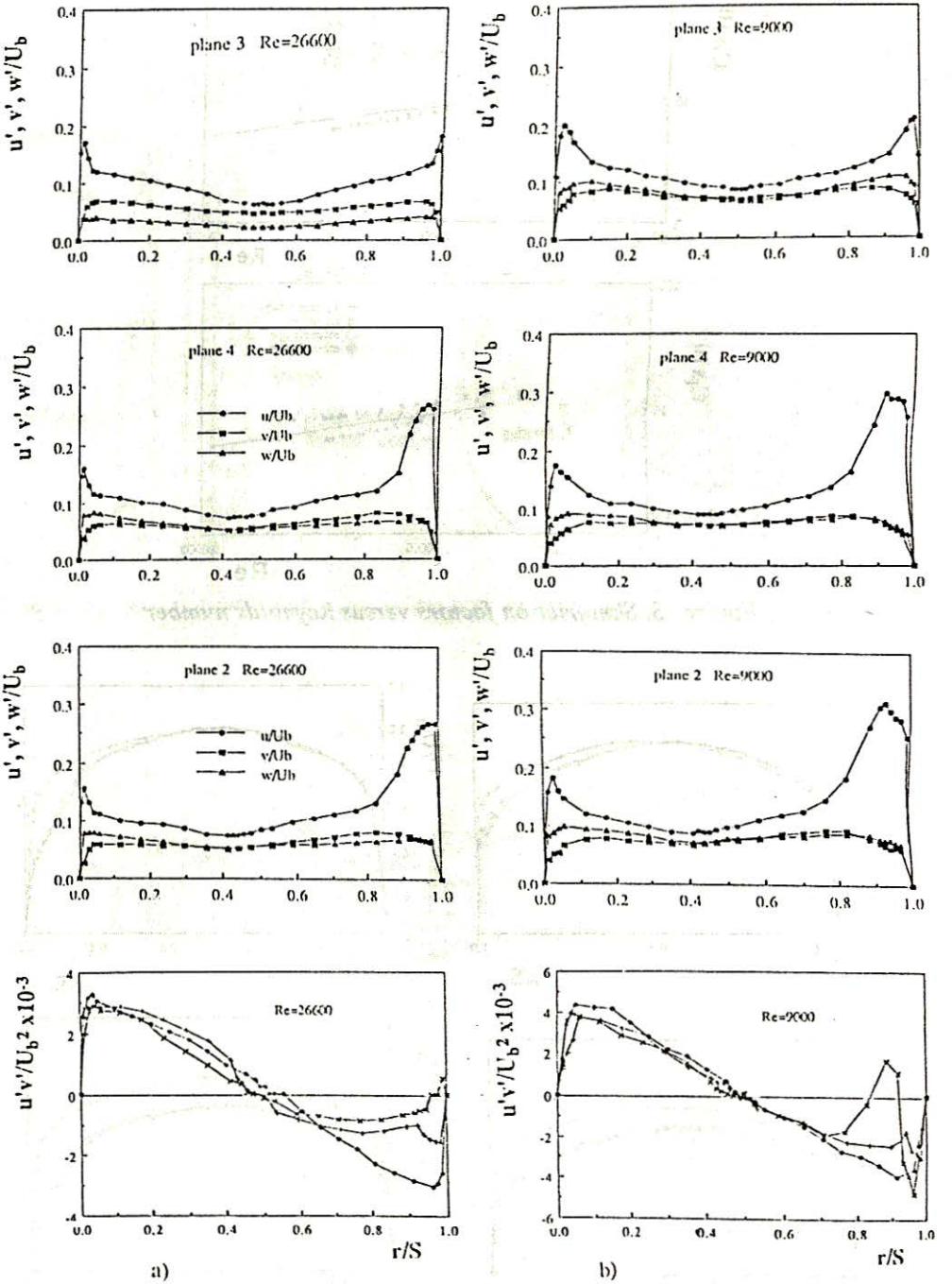

Figure: 5. rms velocity fluctuations and u'v' cross correlation; a) Re = 26600, b) Re = 9000 ● u', ■ v', ▲ w', x plane 2, ◆ plane 3, + plane 4

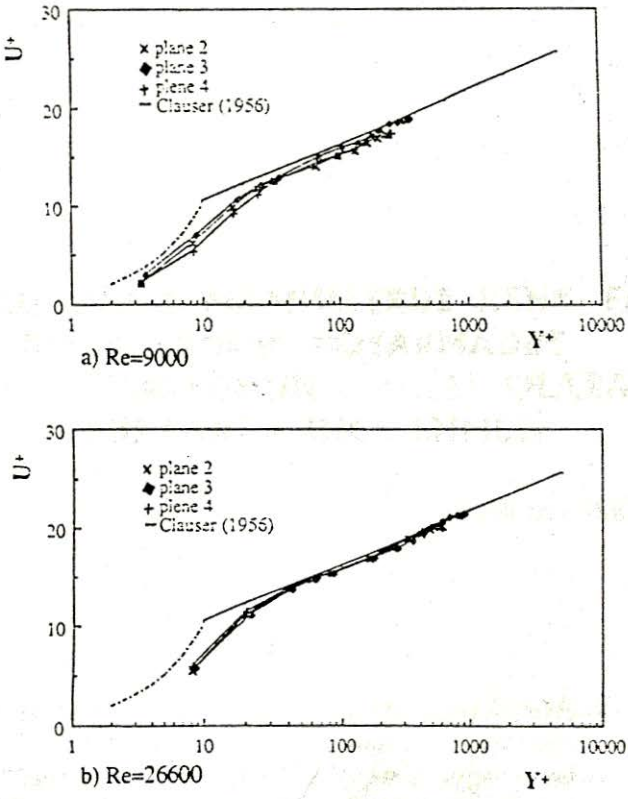

Figure: 6. Velocity profiles in Clauser coordinates

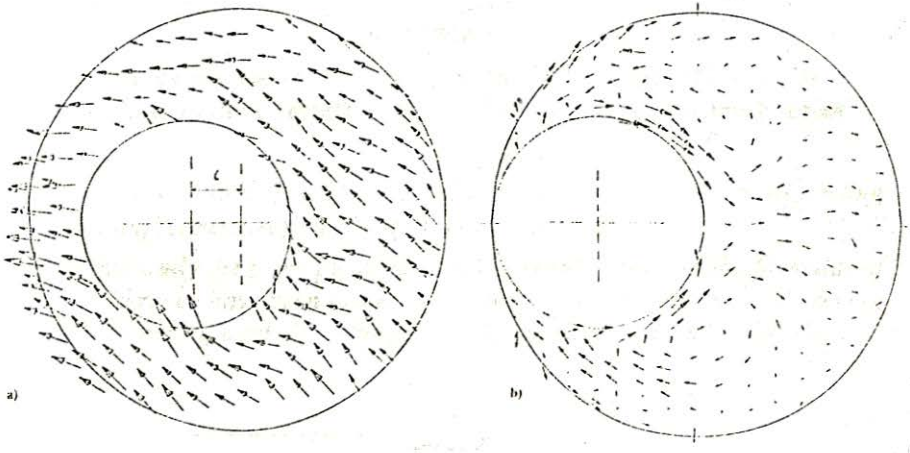

Figure: 7. Secondoray flow velocities
a) eccentricity of 0.5, b) eccentricity of unity